GEOPHYSICS, VOL. 56, NO. 5 (MAY 1991); P. 712–723, 10 FIGS., 5 TABLES.

The generalized gravity anomaly: Endoscopic microgravity

J. Lakshmanan*

ABSTRACT

Various underground 3-D gravity surveys have necessitated a generalization of the usual gravity corrections and of the Bouguer anomaly. The method presented here compares raw, time-dependent gravity measurements, to a model's total theoretical field, including known fields: moon, sun, 1967 Reference Ellipsoid, oceans; partially known fields: due to a single digital terrain model of known geometry but of unknown densities; and unknown fields due to underground structures of unknown shapes and of unknown densities.

For a single-density model, the corresponding first-degree residual is close in concept to the Bouguer anomaly. To best determine underground structure, generalized inversion then leads to determination of the one or several densities and of one or several "regional" parameters, which minimize residuals.

The suggested method is mainly advantagous in special types of gravity surveys, such as rugged terrain, or in the case of underground surveys, where conventional corrections, with a preset terrain density can possibly lead to substantial errors.

Two field examples are developed (1) the Cheops pyramid survey, where the processing of gravity measurements inside, above, and around the pyramid led to an evaluation of the structure's overall density and of density changes in the structure; and (2) the Coche hydroelectric tunnel in the Alps, where the method leads to a 3-D model explaining the very strong gravity anomalies observed in the tunnel and on the mountain above it.

INTRODUCTION

Several underground microgravity surveys have been carried out since 1986. The most spectacular were the four surveys made inside, around, and on the surface of the Cheops Pyramid, Egypt (Lakshmanan and Montluçon, 1987; Bui et al., 1988). Other underground surveys were made in the Coche hydroelectric tunnel, France (Lakshmanan, 1988), and in the Blaisy-Bas and Breval railway tunnels, France.

A common target of these types of underground microgravity surveys is a cavity or a small, low-density zone that may be located either *above* or *below* the gravity stations. The topography may be very severe and the tunnel may be very deep, with measurements both in the tunnel and on the ground surface. The main aims of conventional Bouguer and terrain corrections, i.e., to make stations read at (slightly) differing altitudes comparable, are unsatisfactory. Gravity stations are vertically as well as horizontally, distributed and some stations are within, beneath, or close to anomalous masses. The usual questions are not well satisfied:

What "datum plane" should be used for data reduction?

What correction density should be used for the Bouguer and the terrain corrections?

What hills should one chop off for the terrain corrections?

What valleys should one "fill in"?

We reconsidered the whole set of corrections from the start and defined a new type of gravity anomaly. The "generalized" gravity anomaly is simply the difference between measured gravity and the effect of a given earth model.

Note that when conventional terrain corrections are made up to a sufficient distance, there is a convergence between the new, first-degree, single-density, generalized gravity anomaly and the classical Bouguer anomaly.

As compared to gravity modeling made with the free-air

Presented at the 58th Annual International Meeting, Society of Exploration Geophysicists.
Manuscript received by the Editor July 20, 1989; revised manuscript received October 16, 1990.
*CPGF Horizon, 12 Rue de Paris, 78230 Le Pecq, France.

anomaly as a start, the main additions made by the suggested technique concern (1) use of the generalized inversion method (Tarantola, 1987) to calculate the optimum density, or densities; (2) combination of underground gravity stations and of vertical gradient measurements with the usual surface gravity measurements; and (3) use of a single digital terrain model for all of the gravity stations.

DESCRIPTION OF PROPOSED METHOD

Definition

The procedure described here is applied to a set of 3-D gravity measurements made in, above, under, and around a finite body, and it can be extended to take account of the whole earth. The method compares raw gravity with the sum of the influences of all bodies, known or unknown. This leads to the generalized inversion of a multidensity model, whose computed gravity field best fits the measured data, taking into account probable experimental errors. These bodies can be:

(1) **Known in shape, size and density**: the effects of the moon, the sun, the 1967 Reference Ellipsoid, the oceans, and even the variations in atmospheric pressure which can be exactly computed.

(2) **Known in shape and size, but not in density**: the "terrain" close to or far from the station.

(3) **Unknown in shape, size and density**: the purpose of gravity surveys is to try to define these unknown bodies.

Equivalent free air anomaly

Let the observed gravity $\underline{\mathbf{g}}_0$ be an $M \times 1$ column matrix, with associated variance σ_g^2. Let the time-dependent factors, the effects of the moon, the sun, the gravimeter's drift, and the variations of atmospheric pressure be $M \times 1$ column matrices $\underline{\mathbf{m}}$, $\underline{\mathbf{s}}$, $\underline{\mathbf{T}}$, and $\underline{\mathbf{A}}$. The first order of corrected observed gravity is

$$\underline{\mathbf{g}}_1 = \underline{\mathbf{g}}_0 - \underline{\mathbf{m}} - \underline{\mathbf{s}} - \underline{\mathbf{T}} - \underline{\mathbf{A}}. \tag{1}$$

It is supposed here that drift is perfectly well known, which is the case for most surveys. However, in certain microgravity surveys where maximum precision is required, extension of generalized inversion to the time domain could improve the control of this parameter, as described in Appendix A.

We now calculate known space-dependent gravity effects due to (1) a "reduced" ellipsoid of same ellipticity as the 1967 Reference Ellipsoid, passing through the deepest point of the oceans (an $M \times 1$ column matrix $\underline{\mathbf{E}}'$) at an arbitrary depth of 12 000 m, and (2) the effect of the oceans' mass (an $M \times 1$ column matrix $\underline{\mathbf{0}}$).

Application of these corrections generates a gravity $\underline{\mathbf{g}}_2$, which is close to the conventional free-air corrected value of gravity:

$$\underline{\mathbf{g}}_2 = \underline{\mathbf{g}}_1 - \underline{\mathbf{E}}' - \underline{\mathbf{0}} \tag{2}$$

The evaluations of $\underline{\mathbf{E}}'$ and $\underline{\mathbf{0}}$ at the measurements points are treated in Appendices B and C.

Equivalent "Bouguer" anomaly

The theoretical gravity field g created by a given terrain model (which is the same for all stations, as opposed to conventional processing in which the model is station-dependent) can be represented as an $M \times 1$ column matrix $\underline{\mathbf{g}}$:

$$\underline{\mathbf{g}} = \underline{\mathbf{f}}\,\underline{\mathbf{d}}, \tag{3}$$

where $\underline{\mathbf{f}}$ is an $M \times N$ matrix of the gravitational influences, of n blocks of unit density, grouped in N sets; and $\underline{\mathbf{d}}$ is an $N \times 1$ column matrix of the unknown densities of the N sets of blocks, associated with an a priori variance σ_d^2.

The influence $\underline{\mathbf{f}}$ of a right rectangular prism is given by Nagy (1966); a better approximation can be attained by using prisms with sloping tops (Olivier and Simard, 1981).

In a first step, where a single unknown density is supposed ($N = 1$), the n blocks are designed to best model the surface topography, as well as the known underground voids. For the surface topography, the starting point of the creation of the blocks can be a digital terrain model, which has to be adjusted by adding small extra blocks, to fit with the elevations of the gravity stations, and if necessary, with the terrain variations close to the stations. The bases of the prisms forming digital terrain model should best fit the "reduced" ellipsoid. In the case of surveys including underground stations, known cavities have to be modeled carefully.

In further iterative steps, where $N > 1$, extra blocks may be necessary to best model geologic structures.

The lateral extent D of the digital terrain model outside the survey zone's center (Figure 1) can be limited in practice so that the effect of the terrain outside the model is negligible.

If $\underline{\mathbf{g}}_D$ is the distance-dependent, theoretical value of $\underline{\mathbf{g}}$ and $\underline{\mathbf{f}}_D$, the associated influence matrix such that

$$\underline{\mathbf{g}}_D = \underline{\mathbf{f}}_D\,\underline{\mathbf{d}} \tag{4}$$

one can define residual gravity $\underline{\mathbf{r}}_g$ as

$$\underline{\mathbf{r}}_g = \underline{\mathbf{g}}_2 - \underline{\mathbf{g}}_D \tag{5}$$

or

$$\underline{\mathbf{r}}_g = \underline{\mathbf{g}}_2 - \underline{\mathbf{f}}_D\underline{\mathbf{d}}. \tag{6}$$

The residual density $\underline{\mathbf{r}}_d$ is defined as

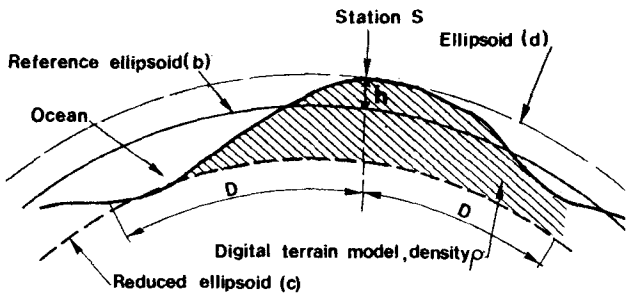

FIG. 1. Sketch of the digital terrain model, the Reference Ellipsoid and the "reduced" ellipsoid.

$$\underline{\mathbf{r}}_d = \underline{\mathbf{d}} - \underline{\mathbf{d}}_0, \tag{7}$$

where $\underline{\mathbf{d}}_0$ is an $N \times 1$ column matrix of the a priori densities of the N sets of blocks.

Using the usual matrix notations (Menke, 1984; Tarantola, 1987), the best density estimate is obtained by the minimization of the sum $S(d)$ of the prediction error (weighted by the a priori standard deviation σ_g) and of the solution's flatness (weighted by the a priori standard deviation σ_d):

$$S(d) = 1/2\{[(\underline{\mathbf{r}}'_g)^t \underline{\mathbf{r}}'_g] + [\underline{\mathbf{r}}'_d)^t \underline{\mathbf{r}}'_d]\} \tag{8}$$

where $\underline{\mathbf{r}}'_g$ and $\underline{\mathbf{r}}'_d$ are $M \times 1$ column matrices, equivalent to $\underline{\mathbf{r}}_g$ and $\underline{\mathbf{r}}_d$, weighted by σ_g and σ_d.

If densities are unconstrained and a constant value of σ_g is assigned to all readings, one has to minimize

$$S'(d) = (\underline{\mathbf{r}}_g)^t \underline{\mathbf{r}}_g = \sum_{i \in I_M} r_g(i)^2. \tag{9}$$

As a first approximation, one can consider that the n blocks are grouped in a single set ($N = 1$) of density d_1 which can be calculated by a least-squares inversion:

$$d_1 = \{(\underline{\mathbf{f}}_D)^t \underline{\mathbf{f}}_D\}^{-1} \{(\underline{\mathbf{f}}_D)^t \underline{\mathbf{g}}\}. \tag{10}$$

Then compute a first "unexplained" or "residual" anomaly $\underline{\mathbf{g}}_3$ related to this particular, single-density model:

$$\underline{\mathbf{g}}_3 = \underline{\mathbf{g}}_2 - \underline{\mathbf{f}}_D d_1. \tag{11}$$

The column matrix $\underline{\mathbf{g}}_3$ is the difference between the equivalent "free-air" corrected gravity and the field due to a terrain of uniform gravity located between the ground and the "reduced" ellipsoid.

If the distance D were extended around the world, $\underline{\mathbf{g}}_3$ would be equal to the Bouguer anomaly, under the conditions that (1) the latter had been computed with density d_1 (with a $4\pi K d_1 z$ plateau correction), (2) terrain corrections had been computed around the world, and (3) corrections had been made for the oceans. In practice, the distance D will be limited to a value such that the horizontal and vertical gravity gradients due to the effects of more distant, ignored zones are negligibly small when compared to the precision of the survey. Thus, for a small microgravity survey covering 100 m by 100 m with slightly irregular topography, the digital terrain model may reach 1 km by 1 km. On the other hand, for a gravity survey for hydrocarbon exploration, one may need to reach 500 km by 500 km.

Equivalent "terrain" correction

To help compare the results with those obtained conventionally, an equivalent terrain correction $\underline{\mathbf{C}}_T$ can be computed by subtracting the total value of the model influences from the conventional value of the slab correction:

$$\underline{\mathbf{C}}_T = 2\pi K d_1 \underline{\mathbf{z}} - \underline{\mathbf{f}}_D d_1, \tag{12}$$

where $\underline{\mathbf{z}}$ is the $M \times 1$ column matrix of elevations and d_1 is the constant density computed by equation (10).

"Geometrical" or "regional" anomalies

The first Bouguer-type model can be made more sophisticated by introducing a "regional" or "geometrical" variation of gravity. Such a variation will account for anomalies which are too strong to be neglected, but the sources of which are too far or too deep to be modeled correctly. One can then compute a second residual anomaly $\underline{\mathbf{g}}_4$ related to this model:

$$\underline{\mathbf{g}}_4 = \underline{\mathbf{g}}_2 - \underline{\mathbf{f}}_D \underline{\mathbf{d}} - \underline{\mathbf{a}}^t \underline{\mathbf{X}}, \tag{13}$$

where $\underline{\mathbf{X}}$ is a $1 \times \ell_{\max}$ row matrix representing various powers of coordinates x, y, z, and $\underline{\mathbf{a}}^t$ is a $k_{\max} \times 1$ column matrix representing the unknown coefficients a_k of X_k.

Modeling can be pursued by keeping $N = 1$, setting the maximum power $\ell_{\max}$ of x and y at 3, and limiting the power of z to 0 or 1. When a large area has to be processed, it is preferable to evaluate the "regional" anomaly with a moving-window inversion. Inside a large window (e.g., a radius of 50 km), one sets $N = 1$ (single density model) and $\ell_{\max} = 1$ (plane regional). Generalized inversion then computes for *each station* an optimum density and the regional components $\delta g/\delta x$ and $\delta g/\delta y$. This is preferred to fitting with high-order polynomials. For the vertical component, it is rarely possible to let them vary freely, unless (z, x) and (z, y) are sufficiently independent variables. In some cases it may be necessary to limit $\delta g/\delta z$ at an arbitrary value (which can reach ± 10 μGal/meter), so that the values of computed densities are geologically acceptable. Generally at this stage the sum $S'(d)$ to be minimized, as well as the average values of $\underline{\mathbf{g}}_4$ as compared to $\underline{\mathbf{g}}_3$, are strongly reduced, but a satisfactory geologic model remains to be constructed.

Multidensity models

The previous model can be geologically and mathematically improved by gradually increasing the number of densities N, while simultaneously decreasing the length $\ell_{\max}$ of the vector $\mathbf{X}$. The final model should attain $\ell = 0$. The last $S'(d)$ is limited by the experimental errors. The density matrix $\underline{\mathbf{d}}$ will be given by

$$\underline{\mathbf{d}} = \{(\underline{\mathbf{f}}_D)^t \underline{\mathbf{f}}_D\}^{-1} \{(\underline{\mathbf{f}}_D)^t \underline{\mathbf{g}}\}. \tag{14}$$

Variable block-size inversion

If the adjustment of the shapes and sizes of the N sets of blocks is made manually, densities are computed by equation (14). However, if one wants to adjust the limits between sets of blocks automatically, then the problem is no longer linear. It can be made pseudolinear by fixing densities at values previously computed and by solving a set of equations linear in df, f being the horizontal or vertical size of the initial block and df its possible adjustment. Alternatively, a nonlinear iterative inversion can be used.

The inversion can also be made in independent steps, starting with a large block structure, then inverting a medium block structure, and ending with a small block structure. At each step, the final, unexplained residuals obtained in the previous step are used as a start to the next inversion.

In the same way, when the data set is too large, overlapping, moving-window techniques can be used without reducing the inversion's quality.

FIELD RESULTS

The suggested method has been applied successfully at several sites. These sites are surface surveys on regular or irregular ground, including sites which compared conventional terrain corrections and the results of the suggested method, over a large area for petroleum exploration, as well as for a microgravity survey. However, the main field of application is underground gravity surveys; the method was initiated after the Cheops pyramid survey. Several hydroelectric and railway tunnels have been investigated with the method. The results obtained at the Cheops pyramid and at the Coche tunnel are described.

The Cheops pyramid in Egypt

The purpose of the first two microgravity surveys was to locate possible secret chambers close to accessible tunnels (Lakshmanan and Montluçon, 1987). Processing of data acquired at different elevations inside the structure led me to consider the meaning of terrain corrections, and led to two further surveys with measurements on and around the pyramid. Between 1986 and 1988, a total of 719 gravity stations were acquired, covering the four slanting edges, the summit, all accessible tunnels, and surrounding ground.

While the archaeological and structural results have been published (Bui et al., 1988), we comment on some of the physical implications of the suggested method.

In a first step, the terrain model was supposed to be homogeneous. The inversion led to an average density of 2.1 g/cm^3 with an average square difference of 329.3 μGal between measured and calculated gravity (while the mean square average free-air anomaly was 1150 μGal). Another model supposed three density zones: the pyramid, the granite covering part of the chambers, and the bedrock. Inversion led to densities of 2.05, 2.81, and 2.25 g/cm^3, respectively. The high value for the granite compared to the usual 2.67 g/cm^3 suggests that its real volume is 5 percent higher than previously believed.

After a series of adjustments, the pyramid was divided into 25 blocks and the bedrock into eight blocks. In addition, a linear regional effect was included in the list of unknowns. The mean square difference was brought down to 25.1 μGal. The results are shown in Figure 2, with a low density (1.9 to 2.0 g/cm^3) summit and various low and high (2.1 to 2.4 g/cm^3) density zones below.

A final adjustment was made by dividing the heart of the pyramid (where most of the data were located) into 17 extra blocks. The mean square difference was brought down to 20.3 μGal, not far from the repeatibility error (8 μGal).

The Coche hydroelectric tunnel

The tunnel located in the French Alps, is 1,300 m long, and passes through a schist overthrust zone. Large quantities of soluble gypsum have been discovered close by. The objective of the survey was to investigate whether the dissolution cavities were near the tunnel, behind its steel lining. Gravity measurements were made along a central line in the tunnel and on the mountain, 200 m above the tunnel. In eight appropriate locations in the 4 m diameter tunnel defined by initial evaluation, three vertical gradient and two horizontal gradient stations were measured, using temporary steel structures.

The initial regression of all 139 measurements led to an abnormally high apparent density (σ = 2.8 g/cm^3) and a very strong regional gradient. To bring down the average density, an abnormal vertical gradient was empirically input in certain models (0.298 mGal/m instead of 0.3086 mGal/m). Fig-

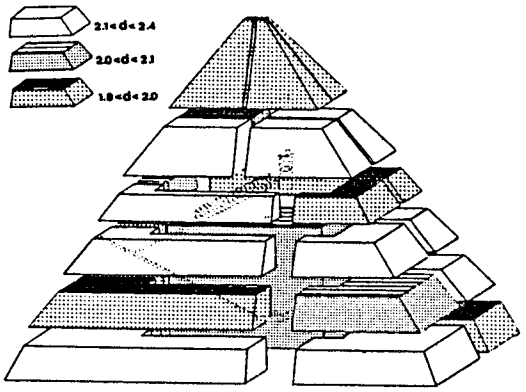

FIG. 2. Densities of the large block structure of the Cheops Pyramid.

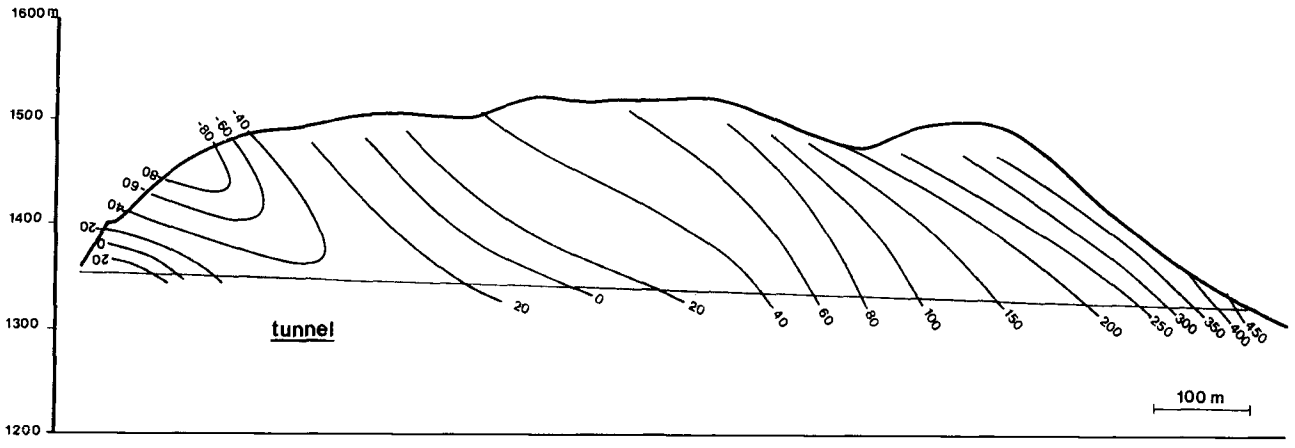

FIG. 3. La Coche tunnel: single density model, residual anomalies (10^{-2} milligals).

ure 3 shows a vertical section and the equivalent Bouguer anomaly in this plane. Table 1 summarizes the results of the various models considered.

The final nine-density model (Figure 4) explains most of the high-frequency anomalies and practically all the regional effect. No abnormal vertical gradient is needed. A tenth, deep block would be needed to remove the last anomalous first-degree regional.

Note in Figure 4 that each of the 3-D blocks of the density model is of a different lateral extent, since the mountain crossed by the Coche tunnel is dome shaped.

DISCUSSION OF GRAVITY CORRECTIONS

Free-air gradient and latitude corrections

Generally, free-air and latitude corrections are considered separately. Their definitions are well established (Nettleton, 1939) and normally use linear approximations of $\delta g/\delta h$ and of $\delta g/\delta\phi$, where g is the gravity field at an elevation h above sea level and at a latitude ϕ. In reality these gradients are two partial derivatives of the Earth's theoretical field.

At sea level, this field has been defined as the effect (attraction + rotational effect) of the 1967 Reference Ellipsoid (Int. Union Geod. Geophysics, 1970). This definition does not include a formula to calculate the gravity values at other altitudes.

Starting from the work of Heiskanen and Moritz (1967), I have derived a general formula, yielding the value of gravity at any point (ϕ, h). This derivation is given in Appendix B. Using this extended formula at $h = 0$, one finds the same values as those published (Int. Union Geod. Geophysics, 1970). The free air gradient of the theoretical field can be computed at any latitude and at any altitude by differentiation (Appendix B).

All measured departures from the gravity and vertical gradient fields predicted by the 1967 Reference Ellipsoid (Karl, 1983, LaFehr and Chan, 1986) are due to large or small anomalous volumes and masses and should *not* be corrected during data reduction.

If one uses the 1967 Reference Ellipsoid, the vertical derivative of its gravity field should also be used since variations can be significant for high mountains.

Bouguer and terrain corrections

We consider (see Figure 1) (a) The real earth partially covered by the oceans and on whose irregular surface is located a measurement point P, where the value of gravity observed is g; (b) the 1967 Reference Ellipsoid, which can be above or below the surface of the real earth; (c) my "reduced" ellipsoid of same ellipticity but located below the deepest oceans (at an arbitrary depth of 12 000 m); and (d) an ellipsoid of the same ellipticity passing by point P.

Table 1. Summary of results for 6 successive density models at the Coche tunnel.

Model	Vertical gradient	Average density	Mean square difference (μGal)
Single density	−0.3086	2.705	651.5
Single density	−0.2980	2.545	618.4
7 densities, 1st degree regional	−0.3086	2.818	150.9
7 densities, 2nd degree regional	−0.3086	2.739	21.6
7 densities, 2nd degree regional	−0.2980	2.536	17.6
9 densities, 1st degree regional	−0.3086	2.561	18.2

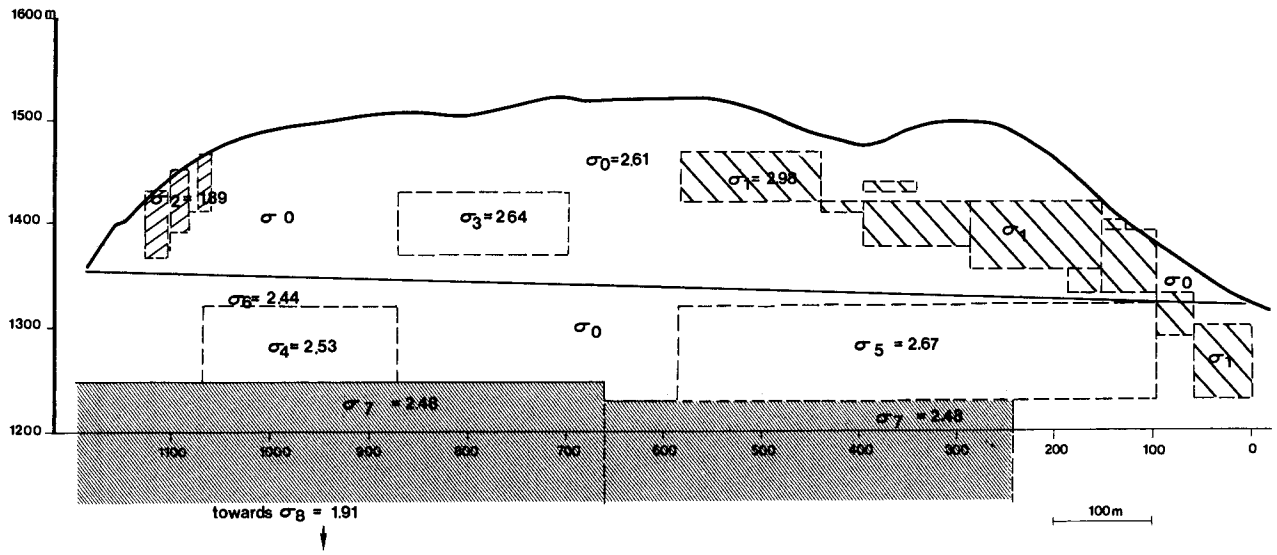

FIG. 4. La Coche tunnel: nine-density model.

Once we have deducted from gravity the influence of (b) (or as I suggested of "reduced" ellipsoid (c), as evaluated in Appendix C), we are left with an irregular thin shell surrounding the earth completely, since the ellipsoids (b), (c), and (d) are symmetrical and concentric. The advantage of replacing the Reference Ellipsoid by a "reduced" ellipsoid is that the gravity effect of the volume located between it and the surface is positive, whether the volume is filled with earth or water.

To correct for the effect of mass outside the "reduced" ellipsoid, four different approaches can be considered.

Flat earth Bouguer correction.—This correction has the value $2\pi G\rho h$ and is supposed to take into account the effect of a horizontal slab of density ρ located between point P at an altitude h and the ellipsoid, G being the universal gravitational constant. This slab correction is then adjusted by subtracting calculated "terrain correction" from it, to account for the effect of lateral topographic changes.

Spherical cap Bouguer corrections.—Several authors (Lejay, 1947; Schleusener, 1954) have shown the fundamental defect of the flat earth correction. For a homogeneous, spherical earth, the correction should be $4\pi G\rho h$, which all professional geophysicists know will lead to large overcorrections. To get away with this paradox, Schleusener (1954) showed that if the correction was made up to the edges of a spherical "cap" (Figure 5) having a radius of 167 km, then the limited spherical correction is $2\pi G\rho h$. Therefore the slab correction is kept at $2\pi G\rho h$ and terrain corrections are carried out up to a radius of 167 km. It is, however, clear that this reasoning, if practically satisfactory, is purely empirical. In fact if one puts the slab correction at its right value of $4\pi G\rho h$, the terrain correction corresponding to the topography beyond 167 km is systematically worth $4\pi G\rho h - 2\pi g\rho h = 2\pi G\rho h$.

Complete spherical corrections.—The more correct, even if only purely theoretical way, of explaining these discrepancies follows. We should first correct for the thin shell separating ellipsoids (d) and (b) [or preferably (d) and (c)], using a value of $4\pi G\rho h$ [or $4\pi G\rho(h + 12\,000)$]. We should then make a large number of terrain corrections related to the differences between the real earth and ellipsoid (d). Since we would be making these corrections around the whole world, and since the percentage of oceans is on the order of 70 percent, we would deduct large values from the full "shell" Bouguer correction worth $4\pi G\rho h$, leading to a net correction (Bouguer − terrain), on the order of 1.7 to $1.9\pi G\rho h$, quite coincidentally on the same order as the net corrections made with a flat earth or with a spherical cap (Figure 6). I consider this approach the soundest theoretically but it is profoundly impractical.

Free-air modeling.—In rugged terrain, data may not be reduced to a horizontal datum, since anomalous masses are possibly located above the selected datum. In such a case, it is therefore practical to limit data reduction to free-air gradient and latitude corrections. The free-air anomaly thus obtained can then be used directly as a starting point for gravity modeling.

In conventional gravity processing, one subtracts the Bouguer slab correction C ($2\pi G\rho h$) from the "free-air" corrected value of gravity and then removes from C terrain correction AC (Figure 6). With the suggested method, one compares the "free-air" corrected value of gravity to the "influence" of the terrain (between the surface and the "reduced" ellipsoid) which is represented by point F in Figure 6. The larger the radius up to which the terrain's influence is calculated, the higher point F will be. If both "terrain" corrections and "influence" evaluations were made around the entire world, then points B and F will coincide in Figure 6.

Comparison between conventional terrain corrections and the suggested method

Figure 7 shows that the conventional terrain correction is station-dependent. For station A, the terrain model for Bouguer slab plus terrain corrections is different from the terrain model corresponding to station B, even if one has extended the corrections as far as possible, as pointed out by LaFehr et al (1988). With the suggested method, the station dependance of these corrections disappears, because a single digital terrain model is used for the whole survey.

For a small microgravity survey, the base of the terrain model needs not be the curved, "reduced" ellipsoid and can be approximated by a plane. In such a case, use of the exact value of the earth's gravity field at each point, as suggested, will make insignificant changes compared to the usual approximation of its vertical and south-north gradients. The main

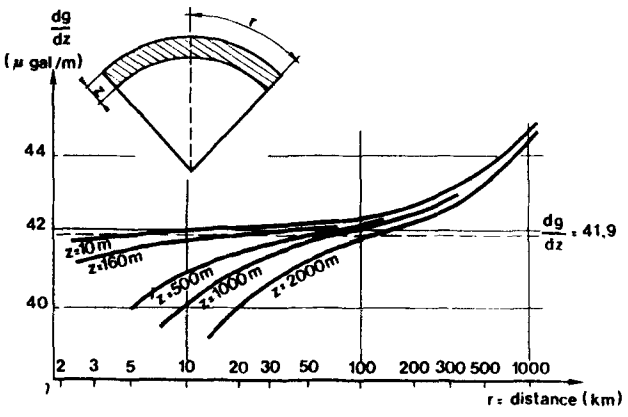

FIG. 5. Gravity effect of a spherical "cap," (after Schleusener (1954)).

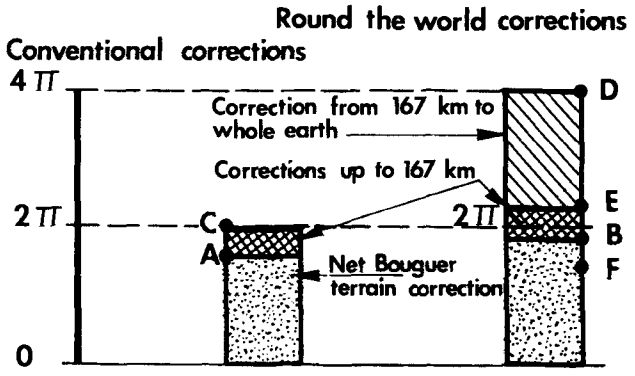

FIG. 6. Relative weights of conventional and "worldwide" corrections.

difference in all cases is the one due to the unicity of the terrain model used for all stations in the suggested method. To compare the application of conventional terrain corrections fully with the suggested method, I have set up a theoretical model resembling the pyramid of Cheops. Let a pyramid, 160 m high, with a homogeneous density of 2 g/cm^3 modeled by three square prisms, be set up on a horizontal plateau (see Figure 8) and let [4], [3], [2] and [1] be gravity stations measured on top and inside the pyramid, considering stations [4] on top of the pyramid at an elevation of 160 m.

With conventional corrections, one would first correct for an infinite slab 160 m thick and then correct for the actual shape up to a certain distance R. If this radius is not infinite (which is never the case in practice), this means that outside distance R, one has created a fictitious infinite slab, 160 m thick.

For station [1], at the base of the pyramid, i.e., at the same elevation as the surrounding plateau, the conventional corrections would be correct whatever the radius R. On the contrary, the suggested method uses a correct terrain model

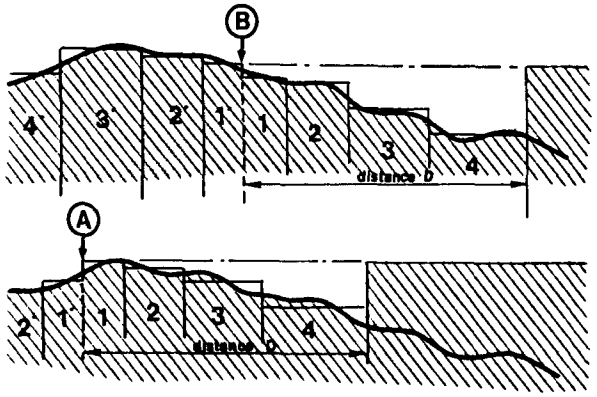

FIG. 7. Terrain model actually used with conventional plateau and terrain corrections.

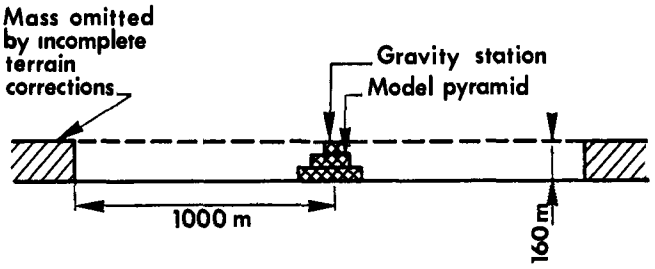

FIG. 8. Theoretical terrain model around the Cheops pyramid.

for all four stations. This is shown numerically by Table 2 (values in microgals).

Table 2 shows that the conventional method leads to large errors for stations at elevations which differ greatly from those of the surrounding ground. For the station at the top of the pyramid, the error (in microgals) would be as shown by Table 3. Note that these errors would considerably increase in the case of an incorrect evaluation of the pyramid's density. An error of 10 percent on the density would lead to an additional correction error of 799 μGal.

From these errors, I developed the suggested method, which compares the free-air anomaly with the influence of a terrain model computed with a unit density. The test model showed that the errors which would have occurred using conventional terrain corrections would have been large in the case of the Cheops pyramid, and therefore processing was limited to the suggested method. In addition, the number of prisms needed for conventional terrain corrections would have been 30 times larger than with the suggested method. This was also the case for the Coche tunnel described above.

A comparison of conventional terrain corrections with the suggested method was made for several land surveys. In the case of the Sidi Boulbra nuclear power plant in Morocco, 880 gravity stations were surveyed, set up along a 20 by 20 m grid (see Figure 9). Conventional terrain corrections were made up to a distance of 1 km around each station, with an assumed density of 2.1 g/cm^3. The suggested method establishing a digital terrain model, over a rectangle extending on all sides, 5 km outside the survey area, with a base 30 m below sea level, to fall below the sea bottom in the considered area. After assuming a density of 1.03 g/cm^3 for seawater, data inversion (which simultaneously corrected for a plane regional) led to an optimum ground density of 1.889 g/cm^3. Statistical comparison of terrain corrections (in microgals) are given in Table 4.

A correlation between conventional terrain corrections (C) and those obtained by the suggested method (S) yields the following values:

$$S = 0.89714C + 9.1250,$$

correlation coefficient = 0.9387.

The slope coefficient (0.89714) is very close to the ratio between the two densities: 1.88904/2.10 = 0.89764.

After subtracting the mean difference between the two methods (due to the enlarged size of the terrain model in the case of the suggested method), the differences do not exceed ±17 μGal, with a mean square difference of 6.3 μGal. The differences are due mainly to incorrect corrections by the

Table 2. Comparison of conventional terrain corrections with suggested method for a model pyramid.

Station elevation (m)	Plateau correction (μGal)	Conventional terrain corrections (μGal)				Terrain correction (suggested method) (μGal)	Influence of the pyramid (μGal)
		R = 1000 m	R = 2000 m	R = 3000 m	R = 10000 m		
160	13404	7146	7567	7708	7906	7991	5413
110	9215	4480	4668	4730	4819	4857	4359
60	5027	3959	4006	4022	4044	4053	973
10	838	4999	4999	4999	4999	4999	−4161

conventional method, when closely spaced stations are located at relatively different elevations. These differences are not negligible: the residual anomalies, related to low-density sand lenses which are the targets of the survey, have an amplitude on the order of 30 to 50 μGal. In areas of strong elevation gradients (cliffs near the sea coast), the error made could have been quite appreciable.

Table 3. Errors made by conventional corrections for a model pyramid.

Distance (m)	Error (μGal)	Error (percent)
1 000	−845	−10.6%
2 000	−424	−5.3%
3 000	−283	−3.5%
5 000	−170	−2.1%
10 000	−85	−1.1%

The comparison tests led to the following conclusions. For surveys made on regular topography, only minor differences appear. However, my method gives slightly increased accuracy, good density control, and reduced computer time.

For surveys made in mountainous areas or for underground surveys, considerable differences between the two methods can occur, due in some cases to insufficient conventional terrain corrections and in most cases to incorrect density selection for conventional terrain corrections. In such areas, computing time is greatly reduced, particularly when digital terrain models with gridded values of elevations are available.

CONCLUSIONS

The method described here was developed for processing gravity data acquired at varied elevations inside, over and around mountains or manmade structures. Because of its association with 3-D acquisition of gravity data on the surface,

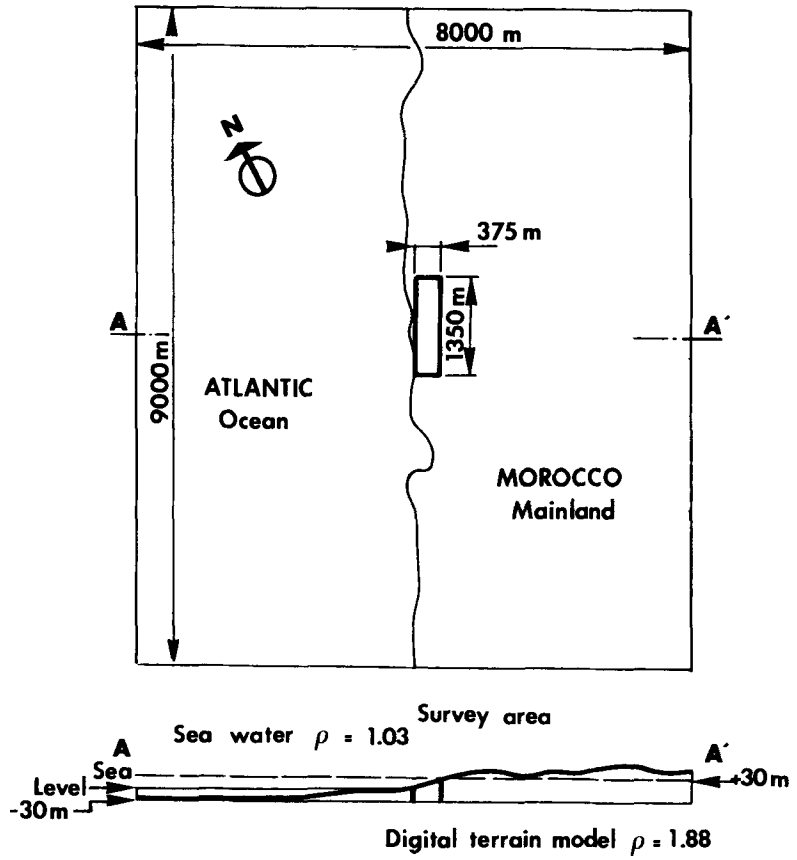

FIG. 9. Digital terrain model used for the Sidi Boulbra nuclear power plant.

Table 4. Comparison between conventional processing and the suggested method at Sidi Boulbra nuclear site (mGal).

	(C) Conventional processing	(S) Suggested method	Difference
Minimum	28.0	106.7	−68.7
Maximum	226.0	306.0	−101.4
Average	55.9	141.4	−85.4
Standard deviation	17.6	16.9	6.1

in tunnels and/or in boreholes, the method has been called endoscopic microgravity. Conventional surveys on flattish ground and borehole gravity surveys are two special cases.

While mainly useful in underground surveys or in regions where severe topographic conditions occur, the method is applicable to all cases of gravity reduction, and is particularly useful for large surveys in areas where digital terrain models are available.

In a first step, it combines the usual latitude and free-air corrections. In a second, it combines in a single correction the slab and the terrain corrections, while selecting an optimum density. This correction is made up to a distance beyond which corrections are negligibly small, using a single digital terrain model for the whole survey. It can also include multidensity inversion.

The method expedites gravity data processing, modeling, and interpretation and can be linked to further inversion techniques such as generalized Nettleton processing, the equivalent source technique, or other linear or nonlinear inversion techniques.

While comparison tests on flattish ground show only minor differences between results obtained with the suggested method and with conventional processing, the differences can be very large in rugged terrain or underground, mainly because of (1) use of a more correct terrain model and (2) selection of an optimum density.

ACKNOWLEDGMENTS

The method described here was developed by Compagnie de Prospection Géophysique Française (CPGF-HORIZON) and, when combined with the corresponding 3-D acquisition of surface and underground data, has been called endoscopic microgravity (EMG). It was developed with support and cooperation from Electricité de France (EDF) to whom credit should be given. The U.S. Corps of Engineers should also be credited for its contribution.

I also thank the Associate Editor and the referees, who have spent much time and efforts to improve both the logic and the legibility of my manuscript.

This paper summarizes the theoretical aspects of my Ph.D thesis (1990) at Institut National Polytechnique de Lorraine (INPL).

REFERENCES

Bichara, M., Erling, J-C., and Lakshmanan, J., 1981, Technique de mesure et d'interprétation minimisant les erreurs de mesure en microgravimétrie: Geophys. Prosp., **29**, 782–789.

Bui, H. D., Montluçon, J., Lakshmanan, J. Erling, J-C. and Nakhla, C., 1988, Les possibilités offertes par la microgravimétrie dans l'auscultation des monuments antiques, Assoc. Int. de Géol. de l'Ing., Symp. Int.: La Géologie de l'Ingénieur appliquée à l'étude, à la préservation et à la protection du patrimoine historique, travaux anciens, sites historiques, Athens, 1063–1069.

Heiskanen, W. A., and Moritz, H., 1967, Physical geodesy: W. H. Freeman and Co.

International Union of Geodesy and Geophysics, International Association of Geodesy, 1970, Geodetic reference system 1967: Bur. Central de l'Assoc. Int de Géodésie.

Karl, J. H., 1983, The normal vertical field of gravity: Geophysics, **48**, 1011–1013.

LaFehr, T. R., and Chan, K. C., 1986, Discussion on "the normal vertical field of gravity": Geophysics, **51**, 1505–1508.

LaFehr, T. R., Yarger, H. L., and Bain, J. E., 1988, Comprehensive treatment of terrain corrections with examples from Sheep Mountain, Wyoming, Presented at the 58th Ann. Int. Mtg., Soc. Expl. Geophys., Expanded Abstracts, 361–363.

Lakshmanan, J., 1988, Applications of Microgravity to the assessment of existing structures and structural foundations: U.S. Corps of Engineers.

——— 1990, Traitement et inversion des données gravimétriques: la microgravimétrie, son application aux recherches de vides: Ph.D. thesis, Institut National Polytechnique de Lorraine, Mémoires Sciences de la Terre, no. 51.

Lakshmanan, J., and Montluçon, J., 1987, Pyramid of Cheops: microgravity weighs the structure and detects cavities: The Leading Edge, **6**, no. 1, 10–17.

Lejay, P., 1947, Développements Modernes de la Gravimétrie: Gauthier-Villars.

Menke, W., 1984, Geophysical data analysis: Discrete inverse theory: Academic Press Co., Inc.

Nagy, D., 1966, The gravitational attraction of a right rectangular prism: Geophysics, **5**, 176–183.

Nettleton, L. L., 1939, Geophysical prospecting for oil, McGraw-Hill Book Co.

Olivier, R. J., and Simard, T. G., 1981, Improvement of the conic prism model for terrain correction in rugged topography: Geophysics, **46**, 1054–1056.

Schleusener, A., 1954, Radius der sphärischen Bouguer-Platte, bei Benutzung des üblichen ebenen Bouguer-Factors 0.0419 mgal/m: Zeits. für Geophys., 29–32, Physica-Verlag.

Tarantola, A., 1987, Inverse problem theory, methods for data fitting and model parameter estimation: Elsevier Science Publ. Co.

APPENDIX A

TIME-DEPENDENT INVERSION

In the case of microgravity surveys, where anomalies in the order of 10 μGal can be significant, near perfect knowledge of the drift curve is necessary. A drift minimization technique was proposed by Bichara, Erling and Lakshmanan (1981). It requires that readings be made in a semirandom order, allowing for iterative adjustment of the lunisolar corrected drift curve.

A more general solution is suggested, by extending equation (8) to the time domain. Let us define the following symbols:

$\underset{\sim}{\mathbf{r}}_l(i)$: a local, high-frequency, spatial residual,
$\underset{\sim}{\mathbf{g}}(i)$: free-air corrected gravity at point (i),
$\underset{\sim}{\tilde{\mathbf{g}}}_l(i)$: average gravity of the four closest stations,
$\underset{\sim}{\mathbf{r}}_u(i)$: residual drift,
$\underset{\sim}{\mathbf{u}}(i)$: unexplained drift and
$\underset{\sim}{\mathbf{u}}_l(i)$: average drift of the four closest stations.

By definition,

$$\underset{\sim}{\mathbf{r}}_l(i) = \underset{\sim}{\mathbf{g}}(i) - \underset{\sim}{\tilde{\mathbf{g}}}_l(i), \tag{A-1}$$

and

$$\underset{\sim}{\mathbf{r}}_u(i) = \underset{\sim}{\mathbf{u}}(i) - \underset{\sim}{\mathbf{u}}_l(i). \tag{A-2}$$

The optimum drift curve is the one which simultaneously minimizes the weighted mean squares of $\underset{\sim}{\mathbf{r}}_l(i)$ and of $\underset{\sim}{\mathbf{r}}_u(i)$. Equation (8) can be generalized to the time domain:

$$S(d) = 1/2\{[(\underset{\sim}{\mathbf{r}}'_g)^t \underset{\sim}{\mathbf{r}}'_g] + [(\underset{\sim}{\mathbf{r}}'_d)^t \underset{\sim}{\mathbf{r}}'_d] + [(\underset{\sim}{\mathbf{r}}_l)^t \underset{\sim}{\mathbf{C}}_l{}^{-1} \underset{\sim}{\mathbf{r}}_l] + [(\underset{\sim}{\mathbf{r}}_u)^t \underset{\sim}{\mathbf{C}}_u{}^{-1} \underset{\sim}{\mathbf{r}}_u]\}, \tag{A-3}$$

where $\underline{r}'_g$ and $\underline{r}'_d$ are the same matrices as those in equation (8) and $\underline{C}_l$ and $\underline{C}_u$ are the matrices of a priori variances and covariances of the "local" spatial residual and of the residual drift, respectively.

Presently densities and drift are alternatively adjusted to attain a "good" solution, when the drift curve is as smooth as possible, while the aliasing effects are no longer visible on the gravity profiles and maps.

APPENDIX B

EFFECT OF 1967 REFERENCE ELLIPSOID WITH LATITUDE AND ELEVATION

At geographic latitude ϕ and on the surface of the ellipsoid, the normal gravity is given by (Int. Union Geod. Geophysics, 1970):

$$g = g_e \frac{1 + k \sin^2\phi}{\sqrt{1 - E^2 \sin^2\phi}}, \tag{B-1}$$

where

g_e = 978.03 184 558 Gals, normal gravity at the equator,
$k = (bg_p - ag_e)/ag_e$ = 0.001 931 663 383 21
b = 6 356 774.5161 m, the semiminor axis of the ellipsoid,
a = 6 378 160.0 m, the semimajor axis of the ellipsoid, and
g_p = 983.217 727 92 Gals, the normal gravity at the pole.

The Int. Union Geod. Geophysics (1970) did not publish any formulas giving the decrease of gravity as a function of elevation. Various simplified formulas or tables of values of the vertical gradient of gravity give an average value of $\delta g/\delta h = -308.6 \pm 0.7$ μGal/m. The variations are related to the elevation and to the latitude.

However, starting from the work of Heiskanen and Moritz (1967), I derived the exact formula giving the theoretical gravity value at any latitude and any elevation above the ellipsoid. Consider the 1967 Reference Ellipsoid, and another ellipsoid exterior to it, but with the same eccentricity ε. Setting $\varepsilon = a\varepsilon'$, the axes of these two ellipsoids are

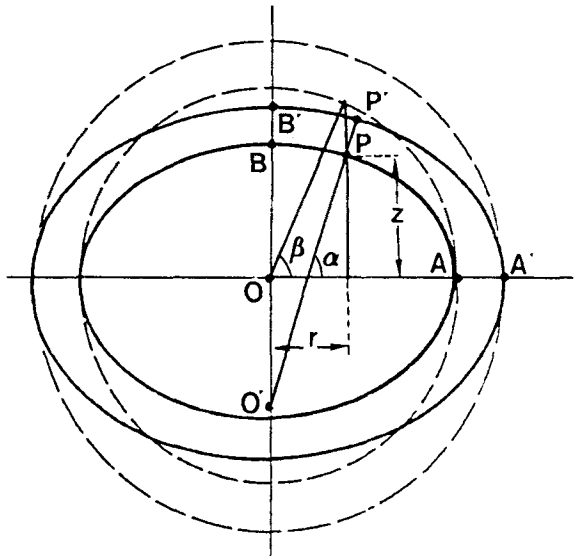

FIG. B-2. Parameters of points P and P' located on concentric ellipsoids.

Ellipsoid	*Semimajor axis*	*Semiminor axis*	
Reference Ellipsoid	$a = \sqrt{b^2 + \varepsilon^2}$	b	(B-2)
Exterior ellipsoid	$a' = \sqrt{b'^2 + \varepsilon^2}$	b'	(B-3)

Coordinates of points P and P', located at the same geographical latitude ϕ, separated by a height h, are given by

$$r = a \cos\beta \tag{B-4}$$

$$z = b \sin\beta \tag{B-5}$$

$$r' = a' \cos\beta' \tag{B-6}$$

$$z' = b' \sin\beta'. \tag{B-7}$$

Because P' is by definition on the same normal O'PP' as P (Figure B-2),

$$r' = a \cos\beta + h \cos\phi, \tag{B-8}$$

and

$$z' = b \sin\beta + h \sin\phi. \tag{B-9}$$

The geographic latitude ϕ, which is the angle between the normal to the ellipsoid through point P and axis OA, is related to "reduced" latitude β, by (Heiskanen and Moritz, 1967, p. 70):

$$\tan\beta = b/a \tan\phi. \tag{B-10}$$

Using equation (B-3), one can calculate β', a', and b' as functions of ϕ, h, a, and b. Defining the parameters

$$r''^2 = r'^2 + z'^2 \tag{B-11}$$

and

$$d''^2 = r'^2 - z'^2, \tag{B-12}$$

one gets

$$b'^2 = r''^2 - \varepsilon^2 \cos^2\beta' \tag{B-13}$$

and

$$b'^2 = (d''^2 - \varepsilon^2 \cos^2\beta')/(2\cos^2\beta' - 1). \tag{B-14}$$

Writing

$$R = r''^2/\varepsilon^2 \tag{B-15}$$

and

$$D = d''^2/\varepsilon^2, \tag{B-16}$$

one gets

$$\cos\beta' = \sqrt{\frac{R}{2} + \frac{1}{2} - \sqrt{\frac{R^2}{4} - \frac{D'}{2} + \frac{1}{4}}} \tag{B-17}$$

and

$$b' = (r''^2 - \varepsilon^2 \cos^2\beta')^{1/2}. \tag{B-18}$$

The general formula of Heiskanen and Moritz (1967) can then be used to calculate the gravity $g(P')$ for point P', located above the 1967 Reference Ellipsoid:

$$g(P') = \frac{1}{W}\left\{\frac{GM}{b'^2 + E^2} + \frac{w^2a^2Eq'}{(b'^2 + E^2)q_0} \cdot \left[\frac{1}{2}\sin^2\beta' - \frac{1}{6}\right] - w^2b'\cos^2\beta\right\} \tag{B-19}$$

where

$$W = \frac{b'^2 + E^2\sin^2\beta'}{b'^2 + E^2}, \tag{B-20}$$

$$q' = 3\left[\frac{b'^2 + E^2}{E^2}\right]\left[1 - \frac{b'}{E}\tan^{-1}\frac{E}{b'}\right] - 1, \tag{B-21}$$

and

$$q_0 = \frac{1}{2}\left\{\left[1 + \frac{3b^2}{E^2}\right]\tan^{-1}\frac{E}{b} - \frac{3b}{E}\right\}. \tag{B-22}$$

Equations (B-20), (B-21), and (B-22) correspond to Heiskanen and Moritz's equations 2.63, 2.67, and 2.58.

G is the universal gravitational constant, M is the earth's mass, GM is the geocentric gravitational constant, $GM = 398\,603 \times 10^9\ m^3/s^{-2}$, and w is the earth's angular velocity of rotation. $7.292\,115\,146\,7 \times 10^{-5}$ rad/s.

For each set of values of latitude and altitude (ϕ, h), one can calculate (β', b') from equations (B-17) and (B-18), and thence, calculate $g(P')$ or $g(\phi, h)$ from equation (B-19). The values of gravity calculated in this way for $g(\phi, 0)$ are exactly those found by Int. Union Geod. Geophysics (1970). For each gravity station located at (ϕ, h), one can directly calculate and subtract the effect of the Reference Ellipsoid from the observed gravity reading.

The vertical gradient of gravity can be calculated by differentiation. At altitude 0, I calculated the "free-air" gradient with the finite difference:

$$\left[\frac{\Delta g}{\Delta h}\right]_0 = \frac{g(100) - g(-100)}{200}, \tag{B-23}$$

where 100 and −100 are altitudes in meters.

Table B-1 summarizes some numerical results, with g expressed in meters/second/second and the free-air gradient in microgals/meter. However, in a very rugged and mountainous terrain, the exact formula giving the gravity value [equation (B-19)] should be used.

Table B-1. Values of gravity and of the free-air gradient at various latitudes and altitudes

Latitude	Gravity	Free-air gradient at h = 0	Free-air gradient at h = 4250 m
0°	9.78031846	−308.779	−308.162
15°	9.78377803	−308.749	−308.132
30°	9.79324019	−308.669	−308.052
45°	9.80619050	−308.559	−307.943
60°	9.81916949	−308.448	−307.833
75°	9.82868902	−308.367	−307.752
90°	9.83217728	−308.338	−307.723

APPENDIX C

GRAVITY FIELD DUE TO THE "REDUCED" ELLIPSOID

Let $S(d)$ be an ellipsoid of same eccentricity ε and concentric to the 1967 Reference Ellipsoid $S(0)$ (see Figure 1), such that $S(d)$ is located slightly below the bottom of the deepest oceans. Let $g[S(0)]$ and $g[S(d)]$ be the gravity field created by these two ellipsoids. $g[S(d)]$ can be calculated by the general equation (B-19) as shown in Appendix B by replacing the earth's mass M by $M - \delta M$, mass of the reduced ellipsoid, where δM is the sum of the mass of the terrain above it, of density σ_0 and of the mass of the seas and oceans of density σ_s.

The volume $V(0)$ of the 1967 Reference Ellipsoid of semimajor axis a, and of semiminor axis b and setting $\varepsilon = a\,\varepsilon'$ is

$$V(0) = \frac{4}{3}\pi ba^2 = \frac{4}{3}\pi b(b^2 + \varepsilon^2).$$

If the two ellipsoids have the same eccentricity ε, then the volume $V(d)$ of the reduced ellipsoid will be

$$V(d) = \frac{4}{3}\pi b'(b'^2 + \varepsilon^2).$$

If the reduced ellipsoid passes the bottom of the deepest ocean, b' can be arbitrarily selected as

$$b - b' = 12\,000\ \text{m}.$$

Then the differential volume δV will be

$$\delta V = V(0) - V(d) = \frac{4}{3}\pi(b - b')(b^2 + bb' + b'^2 + \varepsilon^2),$$

with

$$b = 6\,356\,774.5161\ \text{m}$$

$$\varepsilon = a^2\varepsilon'^2 = 6\,378\,160^2 \times 0.006\,694\,605\,328\,56,$$

or

$$\varepsilon^2 = 2.723\ 427\ 4 \times 10^{11}.$$

Thus, $\delta V = 6.095\ 664 \times 10^{18}\ m^3$.

The mass δM of this volume δV is evaluated as follows. Emerged land represents 29.227 57 percent of the surface of the globe, its average altitude is 850 m, and its average density is supposed to be equal to $\sigma_0 = 2.67$ g/cm^3. Seas and oceans cover 70.772 43 percent of the surface of the globe, with an average depth of 3970 m and an average density of $\sigma_s = 1.030$ g/cm^3. The equivalent average density σ_{app} of the ground between the reference ellipsoid and the reduced ellipsoid will be

$$\sigma_{app} = [(0.707\ 724\ 3 \times 3970 \times 1.030) + (0.707\ 724\ 3 \times (12\ 000 - 3970) \times 2.670) + (0.292\ 275\ 7 \times (850 + 12\ 000) \times 2.67)]/12\ 000,$$

or

$$\sigma_{app} = 2.341\ 289\ \text{g/cm}^3.$$

Since the mass of the earth (or that of the reference ellipsoid) is $M = 5.9737 \times 10^{21}$ T, that of the reduced ellipsoid will be approximately

$$M' = M - \delta M = M - \sigma_{app}\delta V,$$

$$M' = 5.973\ 7 \times 10^{21} - 2.341\ 289 \times 6.095\ 664 \times 10^{18},$$

or

$$M' = 5.959\ 457 \times 10^{21} T.$$

Note that the numerical application of equation (B-19) shows that

$$g(S(0))/g(S(d)) = M/M'$$

(approximately) at sea level, whatever the latitude. An approximately proportionate relationship between the vertical gradients and the masses M and M' is

$$\frac{\delta g[S(0)]}{\delta h} \Big/ \frac{\delta g[S(d)]}{\delta h} = \frac{M}{M'}.$$